

End-to-End Audio-Visual Learning for Cochlear Implant Sound Coding Simulations in Noisy Environments

Meng-Ping Lin,^{1, a)} Enoch Hsin-Ho Huang,^{2, a)} Shao-Yi Chien,¹ and Yu Tsao^{2, 3, b)}

¹⁾Graduate Institute of Electronics Engineering and the Department of Electrical Engineering, National Taiwan University, Taipei 106319, Taiwan

²⁾Research Center for Information Technology Innovation Technology, Academia Sinica, Taipei 115201, Taiwan

³⁾Department of Electrical Engineering, Chung Yuan Christian University, Taoyuan 320314, Taiwan

mplin@media.ee.ntu.edu.tw, enoch.huang@citi.sinica.edu.tw, sychien@media.ee.ntu.edu.tw, yu.tsao@citi.sinica.edu.tw

Abstract: The cochlear implant (CI) is a successful biomedical device that enables individuals with severe-to-profound hearing loss to perceive sound through electrical stimulation, yet listening in noise remains challenging. Recent deep learning advances offer promising potential for CI sound coding by integrating visual cues. In this study, an audio-visual speech enhancement (AVSE) module is integrated with the ElectrodeNet-CS (ECS) model to form the end-to-end CI system, AVSE-ECS. Simulations show that the AVSE-ECS system with joint training achieves high objective speech intelligibility and improves the signal-to-error ratio (SER) by 7.4666 dB compared to the advanced combination encoder (ACE) strategy. These findings underscore the potential of AVSE-based CI sound coding.

[Editor: —]

<https://doi.org/10.1121/10.0042198>

Received: 30 September 2025, Accepted: 22 December 2025, Published Online: 9 January 2026

1. Introduction

The cochlear implant (CI) is a hearing device designed to help individuals with severe-to-profound hearing loss regain partial hearing (Zeng, 2022). The CI system involves an external, upgradable sound processor that uses radio frequency to wirelessly link to a surgically implanted internal device. The CI system transforms speech signals into electrical pulse patterns, which are transmitted via the auditory nervous system to the auditory cortex of the brain, enabling sound perception. Developed through multidisciplinary collaboration, modern CIs now provide impressive speech recognition performance. With well-designed sound coding strategies that translate acoustic signals into electrode stimulation patterns, such as the widely used advanced combination encoder (ACE) strategy (Vandali *et al.*, 2000), most CI users can understand more than 80–90% of speech sentences in quiet conditions (Zeng *et al.*, 2008). However, further improvements are still needed, particularly in the processing of noisy speech.

Speech enhancement (SE) provides a potential pathway for improving CI in noisy environments. With the rapid development of deep learning, SE approaches for CIs are gradually shifting from conventional signal processing algorithms to data-driven neural networks (Henry *et al.*, 2023; Lai *et al.*, 2017; Mamun and Hansen, 2024). Many SE approaches have been applied to CIs, including recent end-to-end architectures (Gajecki and Nogueira, 2025; Gajecki *et al.*, 2023) that integrate both the pre-processing stage and the sound coding strategy (Huang *et al.*, 2021; Wouters *et al.*, 2015), the core component responsible for converting audio into electrical stimuli. However, these audio-only SE (ASE) approaches, which rely solely on audio input, do not make use of the visual cues available for processing background noise and overlapping speech. In general audio applications, audio-visual speech enhancement (AVSE), a common multimodal signal processing approach, has been proposed to incorporate visual information such as lip movements and facial expressions alongside audio signals, and has proven effective in outperforming audio-only speech enhancement methods (Adeel *et al.*, 2021; Chuang *et al.*, 2020, 2022; Hou *et al.*, 2018; Ideli *et al.*, 2019; Michelsanti *et al.*, 2021; Sadeghi *et al.*, 2020). Therefore, the exploration of visual cues and AVSE models for CI sound processing in noisy environments remains an important area of ongoing research (Lai *et al.*, 2025; Tseng *et al.*, 2021).

^{a)}These authors contributed equally to this work.

^{b)}Author to whom correspondence should be addressed.

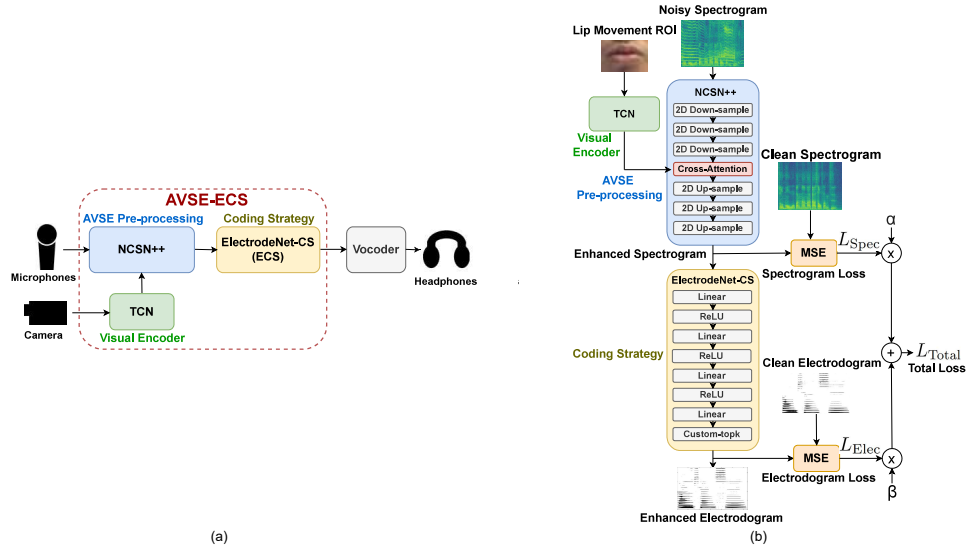


Fig. 1. (a) The architecture of the proposed cochlear implant (CI) system, and the area enclosed by the dashed rectangle indicates the AVSE-ECS network. (b) Overall joint-training architecture for the AVSE-ECS network.

A potential way to improve the CI system using an AVSE module is to integrate it with the ElectrodeNet-CS (ECS) model (Huang *et al.*, 2024). The core signal processing functions of the ACE coding strategy, envelope detection and channel selection (CS), are not differentiable, making them difficult to integrate with neural-network-based AVSE modules and refine through data-driven regression. To overcome this limitation, the ECS model replicates the core signal processing of ACE using a deep neural network (DNN) with a dedicated CS function, achieving comparable performance. Furthermore, the ECS coding strategy enables integration with diverse front-end and post-processing components, as well as joint training and end-to-end optimization. Consequently, the end-to-end AVSE-ECS CI system, which incorporates the AVSE pre-processing module and the ECS model, is proposed and validated using objective evaluations in this study.

This paper is organized as follows. Section 2 explains the proposed AVSE-based CI system. Section 3 describes the experimental setup for objective evaluation. Section 4 offers the results and discussion. Section 5 draws the conclusion.

2. Method

2.1 System Architecture

The system architecture of the proposed AVSE-ECS CI system is illustrated in Fig. 1(a). The AVSE model incorporates auxiliary visual cues to generate enhanced speech, which is further processed by the ECS strategy into electrode stimulation patterns. A tone vocoder (Dorman *et al.*, 2002) is used to convert electrode stimulation patterns into audible speech, which can then be analyzed using objective evaluation methods. Furthermore, this study introduces a joint training approach, and the architecture for training the AVSE-ECS network is illustrated in Fig. 1(b). In this study, three CI network implementations are investigated: ECS (Fig. 2(a)), ASE-ECS (Fig. 2(b)), and AVSE-ECS (Fig. 2(c)).

2.2 Coding Strategy

This study adopts the DNN-based ECS model proposed in (Huang *et al.*, 2024) as the coding strategy, which is the core sound processing of the CI system. This model consists of four dense layers with 1024, 512, 256, and 22 neurons, followed by a custom topk layer designed for the CS function. The ECS model is pre-trained before being integrated into the AVSE-ECS system. Pre-training involved paired spectral-temporal matrices across $L = 65$ bins and $M = 22$ channels derived from clean speech processed with the ACE strategy. The training was configured to preserve key information in the $N_{topk} = 8$ channels selected by the network, while distributing lower envelope data across the remaining $M - N_{topk}$ channels, using the L1 norm across all M channels.

2.3 Visual Encoder

The temporal convolution network (TCN) is employed as the visual encoder as illustrated in Fig. 1. This model consists of a 3D convolutional layer to process temporal sequences of frames, followed by a 2D ResNet-18. The extracted visual features are then passed to the AVSE model as visual embeddings. Note that a modified ResNet-18 visual encoder is pre-trained using the Lip Reading in the Wild (LRW) dataset (Chung and Zisserman, 2016). To provide the most relevant

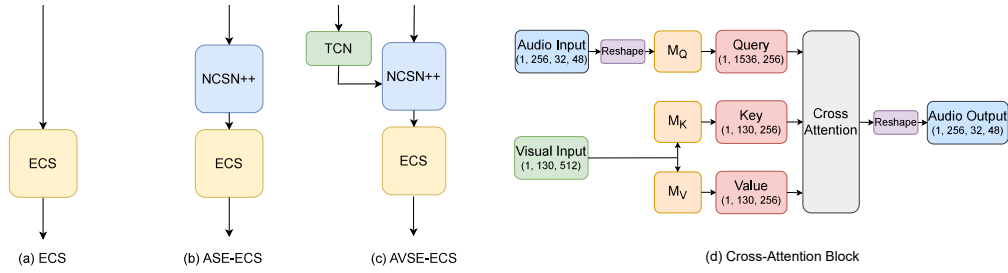


Fig. 2. Neural network implementations: (a) ECS, (b) ASE-ECS, (c) AVSE-ECS, and (d) cross-attention block. As illustrated in Fig. 1, the color blocks represent the modules of ECS (yellow), NCSN++ (blue), and TCN visual encoder (green).

visual cues for SE, the encoder focuses on the mouth, referred to as the region of interest (ROI), rather than utilizing the entire facial region. Facial landmarks are detected using the Mediapipe face tracker (Lugaresi *et al.*, 2019), and the mouth ROI is extracted accordingly. To reduce computational overhead during training, the visual encoder is kept frozen and the embeddings are pre-extracted, minimizing both memory usage and the number of training parameters.

2.4 AVSE Pre-processing

For the AVSE pre-processing, this study adopts and modifies the NCSN++ model from (Song *et al.*, 2021). As this original UNet is designed for generative tasks, the timestep is set to 1 in this study, and the model's output directly serves as the enhanced speech. For audio feature preprocessing before AVSE, the experimental settings are similar to (Lin *et al.*, 2025). Audio signals are resampled to 16 kHz and converted into complex-valued STFT representations. Using a window size of 510 and a periodic Hann window, the resulting frequency dimension is $F = 256$. The hop length is set to 128. Each STFT spectrogram is truncated to $T = 256$ time frames, enabling random cropping during batch training.

2.5 Audio-Visual Fusion

This study explores the use of cross-attention blocks (red block in Fig. 1 (b)) to integrate audio and visual information. The attention mechanism enables neural networks to focus on the most relevant input parts, capture contextual dependencies, and facilitate alignment across modalities. Following a similar approach to (Chen *et al.*, 2024), the self-attention blocks within the UNet architecture are modified by replacing the audio keys and values with visual embeddings generated by the visual encoder. Augmenting the audio input with lip movement information is intended to utilize visual cues to enhance speech reconstruction and thereby improve the overall performance of the SE system. To explain the design of the audio-visual fusion module, the cross-attention mechanism is shown in Fig. 2 (d). Audio features (in blue) and visual features (in green) are provided as input, with dimensions indicated numerically. M_Q , M_K , and M_V represent the transformation layers for query, key, and value, respectively. They are fused by the cross attention block, then reshaped as audio output.

2.6 Joint Training

Joint training, as shown in Fig. 1 (b), simultaneously optimizes both the AVSE pre-processing module (blue block) and the ECS module (yellow block) within an end-to-end framework. To guide the SE module toward generating high-quality enhanced speech during the learning process, a training objective called spectrogram loss is defined as follows:

$$L_{\text{Spec}} = \text{MSE}(\mathbf{E}, \mathbf{C}), \quad (1)$$

where MSE is the mean squared error between \mathbf{E} , the enhanced speech from the AVSE model, and \mathbf{C} , the clean ground truth. To measure the distance for each enhanced-clean electrodiagram pair, the electrodiagram loss is defined as

$$L_{\text{Elec}} = \text{MSE}(\hat{\mathbf{E}}, \hat{\mathbf{C}}), \quad (2)$$

where $\hat{\mathbf{E}}$ is the enhanced electrodiagram from the AVSE-ECS model and $\hat{\mathbf{C}}$ is the clean electrodiagram from the ECS model. The clean electrodiagram is derived from the output of the ECS model when clean speech is provided as input. By narrowing the distance between the clean electrodiagram and the enhanced electrodiagram, the output electrode pattern in AVSE-ECS can be further refined, reducing the impact of input noise and improving speech intelligibility.

By considering L_{Spec} and L_{Elec} concurrently, the total loss is defined as

$$L_{\text{Total}} = \alpha * L_{\text{Spec}} + \beta * L_{\text{Elec}}, \quad (3)$$

where α and β are weights for L_{Spec} and L_{Elec} , respectively.

3. Experiments

This section presents the experimental setups in this study.

3.1 Objective Evaluation Metrics

To assess the performance of CI systems, three commonly-used objective evaluation metrics are employed: short-time objective intelligibility (STOI) (Taal *et al.*, 2011), extended short-time objective intelligibility (ESTOI) (Jensen and Taal, 2016), and normalized covariance measure (NCM) (Goldsworthy and Greenberg, 2004). These metrics estimate speech intelligibility by measuring the correlation between CI-vocoded and clean speech. Furthermore, the neural models are compared using the signal-to-error ratio (SER) (Liu *et al.*, 2015), where the error components include remaining noise after SE processing as well as artifacts and distortions introduced by the SE model.

3.2 Dataset

The audiovisual dataset used in this study is based on the Taiwan Mandarin Hearing in Noise Test (TMHINT) speech material (Wong *et al.*, 2007), which consists of 16 phonemically balanced lists. Each list contains 20 sentences, with each sentence consisting of 10 syllables (Chinese characters). The duration of each utterance ranges from approximately 2 to 4 seconds. The audio-only dataset and the audio-visual dataset are both based on TMHINT sentences. The audio-only TMHINT dataset is used to train the ECS model, as described in (Huang *et al.*, 2024), with the exception that 320 clean sentences from Lists 1 to 8 are used in this study.

For training and inference of the AVSE-ECS system, the Taiwan Mandarin Speech with Video (TMSV) dataset (Chuang *et al.*, 2022), consisting of speech and video recordings of TMHINT sentences, is adopted. The method for using the TMSV dataset is similar to that described in (Chuang *et al.*, 2022). This dataset includes speech recordings from 18 native Mandarin speakers (13 males and 5 females). In this study, considering gender balance, 8 speakers (4 male, 4 female) from TMSV are selected for training and validation. For each speaker with 320 utterances, sentences 1-190 are used for training, and sentences 191-200 for validation. These speech files are mixed with 100 types of noise (Hu, 2004) at five signal-to-noise ratio (SNR) levels (-12, -6, 0, 6, 12 dB). To reduce training time, a total of 12,000 utterances are randomly sampled. For evaluation, utterances 201-320 from two unseen speakers (1 male, 1 female) are used. These are corrupted with five noise types including music, street noise, engine noise, baby cry, and pink noise, and mixed at SNR levels of -1, -4, -7, and -10 dB, yielding a total of 4,800 noisy utterances. The training and testing sets are fully mismatched in terms of speech content, noise types, speakers, and SNR levels to ensure robust generalization.

3.3 Training Configuration

According to the total loss L_{Total} introduced in Section 2.6, two types of training configurations are designed to train the AVSE-ECS Network: pre-trained and joint training. For the pre-trained method, the AVSE model is trained independently and concatenated with ECS. For the joint training method, an untrained AVSE network is connected to ECS, and the training of the full AVSE-ECS network includes the spectrogram loss L_{Spec} and the electrodogram loss L_{Elec} . The pre-trained method can be regarded as a special case of joint training, which only includes L_{Spec} in the training stage by setting $\beta = 0$. Note that in all configurations, the ECS models are pre-trained and concatenated after the AVSE model. During the joint training stage, all the parameters in ECS are frozen, and only the parameters in the AVSE model are tuned.

3.4 Objective Evaluation

The following three experiments are conducted for objective evaluation.

1. ECS with clean and noisy speech
2. AVSE-ECS with different β values
3. Comparison of ACE, ECS, ASE-ECS, AVSE-ECS

In the first experiment, the pre-trained ECS model is evaluated on the TMSV test set using STOI, ESTOI, and NCM metrics under both clean and noisy conditions. All evaluations are conducted on unseen speakers, with the objective scores for the noisy condition averaged over different noise types and SNR levels.

The second experiment examines how model weights in joint training affect speech intelligibility. Following the pre-trained method with $\alpha = 1$, and different β values are studied. The result helps select β for the next experiment.

The third experiment compares three CI network implementations: ECS (Fig. 2(a)), ASE-ECS (Fig. 2(b)), and AVSE-ECS (Fig. 2(c)), with the common ACE coding strategy as the baseline. Apart from the ECS model without the SE function, the ASE-ECS model is an audio-only system in which self-attention replaces the cross-attention mechanism used in the AVSE-ECS model. AVSE-ECS, the proposed end-to-end CI system, is evaluated using both the pre-trained method and the joint training method. For all experiments, α is set to 1, and in the joint training setup, β is set to 0.5.

4. Results and Discussion

4.1 ECS with clean and noisy speech

Table 1. Objective evaluation of the ECS model

Input Speech	STOI \uparrow	ESTOI \uparrow	NCM \uparrow
Clean	0.7604	0.5866	0.6809
Noisy	0.4870	0.2073	0.3258

Table 2. Objective evaluation of the AVSE-ECS network with different β values under noisy conditions

β	STOI \uparrow	ESTOI \uparrow	NCM \uparrow
1.0	0.6196	0.3705	0.5217
0.5	0.6305	0.3899	0.5211
0.25	0.6295	0.3879	0.5199

The overall objective intelligibility of the ECS model under clean and noisy conditions is shown in Table 1. For clean speech, ECS achieves an STOI score of 0.7604, which drops to 0.4870 under noisy conditions, averaged across speakers, noise types and SNR levels. Similar declines in ESTOI and NCM occur as conditions shift from clean to noisy. The ECS model’s performance declines under noisy conditions, as it only simulates the ACE strategy without SE capability.

4.2 AVSE-ECS with different β values

Table 2 presents the objective evaluation results of AVSE-ECS with different joint training setups. In noisy conditions, AVSE-ECS attains STOI scores of 0.6295 ($\beta = 0.25$), 0.6305 ($\beta = 0.5$), and 0.6196 ($\beta = 1$), averaged over speakers, noise types and SNR levels. Similar trends in STOI and ESTOI scores appear across the three β values. These results suggest that emphasizing β , the weight on the electrodoagram loss L_{Elec} , to 1 does not necessarily improve speech intelligibility. On the other hand, a smaller β value of 0.25 limits the refinement of the electrodoagram. Among the tested values, $\beta = 0.5$ results in the highest STOI and ESTOI scores. Although $\beta = 1$ achieves a slightly higher NCM score (0.5217) compared to $\beta = 0.5$ (0.5211), the difference is considerably small. Therefore, the β value of 0.5 is selected for the subsequent experiment.

4.3 Comparison of ACE, ECS, ASE-ECS, and AVSE-ECS

Table 3 compares various CI system implementations under noisy conditions, with objective evaluation scores averaged across speakers, noise types and SNR levels. The ECS model achieves an average STOI score of 0.4870, comparable to the ACE strategy. With the pre-trained setup, the audio-only ASE-ECS model achieves a STOI score of 0.5943, surpassing the ECS strategy without the SE module. Incorporating visual cues in the AVSE-ECS model further increases STOI scores to 0.6141 (pre-trained) and 0.6305 (joint training). Similar trends appear in ESTOI and NCM scores.

The average SER scores for all models are higher than that of the ACE strategy. The SER difference for the ECS model compared to ACE is 0.0761 dB, while the scores for ASE-ECS (3.8075 dB) and pre-trained AVSE-ECS (3.7291 dB) are close to each other. Moreover, the joint-training model achieves the highest SER score, exceeding ACE by 7.4666 dB.

Therefore, integrating ASE and AVSE models improves objective speech intelligibility over the ECS model, while the AVSE-ECS model with visual cues outperforms the audio-only ASE-ECS model in STOI, ESTOI, and NCM scores. In joint training that incorporates the clean electrodoagram as an auxiliary target, the AVSE model can directly generate enhanced electrode stimulation patterns and achieve the highest scores in this study.

4.4 Discussion

This study can be further extended. Beyond the comprehensive objective evaluations, subjective listening tests are planned for the proposed AVSE-ECS method with both normal-hearing participants using CI simulations and actual CI users. Additionally, physiological evaluations, such as responses to auditory stimuli processed by the proposed approaches, may provide further objective evidence in human subjects.

Table 3. Objective evaluation of various CI implementations under noisy conditions

Method	Configuration	STOI \uparrow	ESTOI \uparrow	NCM \uparrow	Δ SER (dB) \uparrow
ACE	-	0.4870	0.2067	0.3262	-
ECS	-	0.4870	0.2073	0.3258	0.0761
ASE-ECS	Pre-trained	0.5943	0.3557	0.4914	3.8075
AVSE-ECS	Pre-trained	0.6141	0.3672	0.5067	3.7291
AVSE-ECS	Joint training	0.6305	0.3899	0.5211	7.4666

In this study, the objective evaluation relies on a single TMSV dataset in one language, Mandarin Chinese. As highlighted in prior studies (Chao *et al.*, 2025; Sankar *et al.*, 2024; Zhang *et al.*, 2019), regression-based tasks such as speech enhancement and speech separation are generally less sensitive to language differences. As a result, models trained on English speech data have shown effective generalization to other languages. Moreover, to ensure the cross-language, cross-speaker, cross-dataset, and cross-validation generalizability of the proposed approach, further studies using diverse datasets are planned. Analyses with a wider range of noise types are to be conducted, as the present results indicate no clear differences among the five noise types examined. Since audiovisual datasets are less accessible than audio-only ones, further dataset collection and development are needed in terms of size, diversity, and real-world coverage. For each dataset, multiple runs with different random seeds will be repeated to ensure the consistency and robustness of the proposed system.

Issues in implementing AVSE in CI hardware need to be tackled. The proposed AVSE system with end-to-end CI processing can be executed on a personal computer, making it suitable for applications with relaxed timing constraints, such as movie streaming, online courses, and playback scenarios. Latency is challenging for real-time deployment on CI sound processors, but integration with external edge devices such as smartphones, tablets, or smart glasses can offload computation from implant-side processors, enabling more advanced audiovisual processing in everyday use. Looking ahead, we plan to reduce the model's computational load through techniques such as pruning and knowledge distillation. Further investigations into the NCSN++ model, the proposed AVSE backbone, will assess lightweight alternatives for hardware implementation and seamless integration into the hearing assistance ecosystem. In the future, advances in device processing power are expected to reduce signal processing latency and make the AVSE module a feasible application.

It is worth noting to consider a number of related topics. A recent study demonstrates an analogous architecture to an end-to-end neural amplifier designed for hearing aids (Ahmed *et al.*, 2025). Therefore, more advanced AVSE pre-processing methods and end-to-end frameworks will be explored to enhance the overall CI sound processing system. Furthermore, the role of multisensory cues in CI perception will be investigated to provide more natural sound and enhance communication and well-being for CI users. Research on deep learning and CI sound processing is an ongoing journey.

5. Conclusion

This paper introduces a novel end-to-end CI system, AVSE-ECS, which integrates an audio-visual speech enhancement (AVSE) model with a deep-learning-based sound coding strategy, ElectroNet-CS (ECS). This system exhibits strong noise suppression capabilities and effectively mitigates severe performance degradation of the CI in noisy environments. Joint training of the end-to-end system enhances electrode stimulation patterns for greater clarity and recognizability, as verified through experiments. Future work includes subjective listening evaluations, cross-dataset generalization studies, and exploration of alternative AVSE preprocessing frameworks. The methods and findings of this study may provide insights into end-to-end CI coding strategies, multimodal processing, and related fields.

6. Author Declarations

6.1 Conflict of Interest

The authors have no conflicts to disclose.

6.2 Ethics Approval

This study was based solely on CI simulations and did not involve human participants, patient data, or animal subjects.

7. Data Availability

The data supporting the results of this research are available from the corresponding author upon reasonable request.

References and links

- Adeel, A., Gogate, M., Hussain, A., and Whitmer, W. M. (2021). "Lip-reading driven deep learning approach for speech enhancement," *IEEE Trans. Emerg. Top. Comput. Intell.* **5**(3), 481–490.
- Ahmed, S., Zezario, R. E., Yuan, H.-G., Hussain, A., Wang, H.-M., Chung, W.-H., and Tsao, Y. (2025). "NeuroAMP: A novel end-to-end general purpose deep neural amplifier for personalized hearing aids," to appear in *IEEE Trans. Artif. Intell.*
- Chao, R., Nasretidinov, R., Wang, Y. C. F., Jukić, A., Fu, S.-W., and Tsao, Y. (2025). "Universal speech enhancement with regression and generative mamba," in *Proc. Interspeech*, Rio de Janeiro, Brazil.
- Chen, C.-W., Hou, J.-C., Tsao, Y., Chen, J.-C., and Chien, S.-Y. (2024). "Davse: A diffusion-based generative approach for audio-visual speech enhancement," in *Proc. 3rd COG-MHEAR Workshop on Audio-Visual Speech Enhancement (AVSEC)*, Dublin, Ireland.
- Chuang, S.-Y., Tsao, Y., Lo, C.-C., and Wang, H.-M. (2020). "Lite audio-visual speech enhancement," in *Proc. Interspeech*, Shanghai, China.
- Chuang, S.-Y., Wang, H.-M., and Tsao, Y. (2022). "Improved lite audio-visual speech enhancement," *IEEE/ACM Trans. Audio Speech Lang. Process.* **30**, 1345–1359.

- Chung, J. S., and Zisserman, A. (2016). "Lip reading in the wild," in *Proc. ACCV*.
- Dorman, M. F., Loizou, P. C., Spahr, A. J., and Maloff, E. (2002). "A comparison of the speech understanding provided by acoustic models of fixed-channel and channel-picking signal processors for cochlear implants," *J. Speech Lang. Hear. Res.* **44**, 1–6.
- Gajecki, T., and Nogueira, W. (2025). "Adversarial learning for end-to-end cochlear speech denoising using lightweight deep learning models," in *Proc. IEEE Int. Conf. Acoust. Speech Signal Process. (ICASSP)*, pp. 1–5.
- Gajecki, T., Zhang, Y., and Nogueira, W. (2023). "A deep denoising sound coding strategy for cochlear implants," *IEEE Trans. Biomed. Eng.* **70**(9), 2700–2709.
- Goldsworthy, R. L., and Greenberg, J. E. (2004). "Analysis of speech-based speech transmission index methods with implications for nonlinear operations," *J. Acoust. Soc. Amer.* **116**(6), 3679–3689.
- Henry, F., Glavin, M., and Jones, E. (2023). "Noise reduction in cochlear implant signal processing: A review and recent developments," *IEEE Rev. Biomed. Eng.* **16**, 319–331.
- Hou, J.-C., Wang, S.-S., Lai, Y.-H., Tsao, Y., Chang, H.-W., and Wang, H.-M. (2018). "Audio-visual speech enhancement using multimodal deep convolutional neural networks," *IEEE Trans. Emerg. Top. Comput. Intell.* **2**(2), 117–128.
- Hu, G. (2004). "100 nonspeech environmental sounds" Available online: <http://www.cse.ohio-state.edu/pnl/corpus/HuCorpus.html>.
- Huang, E. H.-H., Chao, R., Tsao, Y., and Wu, C.-M. (2024). "ElectroNet—A deep-learning-based sound coding strategy for cochlear implants," *IEEE Trans. Cogn. Dev. Syst.* **16**(1), 346–357.
- Huang, E. H.-H., Wu, C.-M., and Lin, H.-C. (2021). "Combination and comparison of sound coding strategies using cochlear implant simulation with mandarin speech," *IEEE Trans. Neural Syst. Rehabil. Eng.* **29**, 2407–2416.
- Ideli, E., Sharpe, B., Bajić, I. V., and Vaughan, R. G. (2019). "Visually assisted time-domain speech enhancement," in *Proc. GlobSIP*.
- Jensen, J., and Taal, C. H. (2016). "An algorithm for predicting the intelligibility of speech masked by modulated noise maskers," *IEEE/ACM Trans. Audio Speech Lang. Process.* **24**(11), 2009–2022.
- Lai, R. L., Hou, J.-C., Chern, I.-C., Hung, K.-H., Chen, Y.-T., Gogate, M., Arslan, T., Hussain, A., Lin, C.-W., and Tsao, Y. (2025). "Leveraging self-supervised audio-visual pretrained models to improve vocoded speech intelligibility in cochlear implant simulation," *IEEE Trans. Biomed. Eng.* To appear.
- Lai, Y.-H., Chen, F., Wang, S.-S., Lu, X., Tsao, Y., and Lee, C.-C. (2017). "A deep denoising autoencoder approach to improving the intelligibility of vocoded speech in cochlear implant simulation," *IEEE Trans. Biomed. Eng.* **64**(7), 1568–1578.
- Lin, M.-P., Hou, J.-C., Chen, C.-W., Chien, S.-Y., Chen, J.-C., Lu, X., and Tsao, Y. (2025). "Bridging the multi-modality gaps of audio, visual and linguistic for speech enhancement," arXiv preprint arXiv:2501.13375.
- Liu, Y., Nower, N., Yan, Y., and Unoki, M. (2015). "Restoration of instantaneous amplitude and phase of speech signal in noisy reverberant environments," in *2015 23rd European Signal Processing Conference (EUSIPCO)*, IEEE, pp. 879–883.
- Lugaresi, C., Tang, J., Nash, H., McClanahan, C., Uboweja, E., Hays, M., Zhang, F., Chang, C.-L., Yong, M. G., Lee, J. et al. (2019). "Mediapipe: A framework for building perception pipelines," arXiv preprint arXiv:1906.08172.
- Mamun, N., and Hansen, J. H. L. (2024). "Speech enhancement for cochlear implant recipients using deep complex convolution transformer with frequency transformation," *IEEE/ACM Trans. Audio Speech Lang. Process.* **32**, 2616–2629.
- Michelsanti, D., Tan, Z.-H., Zhang, S.-X., Xu, Y., Yu, M., Yu, D., and Jensen, J. (2021). "An overview of deep-learning-based audio-visual speech enhancement and separation," *IEEE/ACM Trans. Audio Speech Lang. Process.* **29**, 1368–1396.
- Sadeghi, M., Leglaive, S., Alameda-Pineda, X., Girin, L., and Horaud, R. (2020). "Audio-visual speech enhancement using conditional variational auto-encoders," *IEEE/ACM Trans. Audio Speech Lang. Process.* **28**, 1788–1800.
- Sankar, A., Anand, S., Varadhan, P., Thomas, S., Singal, M., Kumar, S. et al. (2024). "IndicVoices-R: Unlocking a massive multilingual multi-speaker speech corpus for scaling indian TTS," *Adv. Neural Inf. Process. Syst.* **37**, 68161–68182.
- Song, Y., S.-Dickstein, J., Kingma, D. P., Kumar, A., Ermon, S., and Poole, B. (2021). "Score-based generative modeling through stochastic differential equations," in *Proc. Int. Conf. Learn. Represent. (ICLR)*, Virtual Conference.
- Taal, C. H., Hendriks, R. C., Heusdens, R., and Jensen, J. (2011). "A short-time objective intelligibility measure for time-frequency weighted noisy speech," *IEEE/ACM Trans. Audio Speech Lang. Process.* **19**(7), 2125–2136.
- Tseng, R.-Y., Wang, T.-W., Fu, S.-W., Lee, C.-Y., and Tsao, Y. (2021). "A study of joint effect on denoising techniques and visual cues to improve speech intelligibility in cochlear implant simulation," *IEEE Trans. Cogn. Dev. Syst.* **13**(4), 984–994.
- Vandali, A. E., Whitford, L. A., Plant, K. L., Clark, G. M. et al. (2000). "Speech perception as a function of electrical stimulation rate: Using the nucleus 24 cochlear implant system," *Ear Hear.* **21**(6), 608–624.
- Wong, L. L., Soli, S. D., Liu, S., Han, N., and Huang, M.-W. (2007). "Development of the Mandarin hearing in noise test (MHINT)," *Ear Hear.* **28**(2), 70S–74S.
- Wouters, J., McDermott, H. J., and Francart, T. (2015). "Sound coding in cochlear implants: From electric pulses to hearing," *IEEE Signal Process. Mag.* **32**(2), 67–80.
- Zeng, F.-G. (2022). "Celebrating the one millionth cochlear implant," *JASA-EL* **2**(7).
- Zeng, F.-G., Rebscher, S., Harrison, W., Sun, X., and Feng, H. (2008). "Cochlear implants: System design, integration, and evaluation," *IEEE Rev. Biomed. Eng.* **1**, 115–142.
- Zhang, Y., Weiss, R. J., Zen, H., Wu, Y., Chen, Z., Skerry-Ryan, R. J. et al. (2019). "Learning to speak fluently in a foreign language: Multilingual speech synthesis and cross-language voice cloning," in *Proc. Interspeech*, Graz, Austria, pp. 2080–2084.